PHYSICAL REVIEW A VOLUME 55, NUMBER 3 MARCH 1997

Self-induced Bragg-type scattering in dark optical superlattices

Peter Horak and Helmut Ritsch
Institut für Theoretische Physik, Universität Innsbruck, Technikerstr. 25, A-6020 Innsbruck, Austria
(Received 21 August 1996)

We show that the coherent part of the atomic fluorescence spectrum in a dark optical superlattice can be interpreted as a new type of Bragg scattering of the trapping lasers by the periodic atomic distribution. We explicitly solve the 1D problem to demonstrate that this built-in mechanism provides a diagnostic tool to determine the atomic position and energy distribution without any extra disturbance of the system. Hence, in principle, this method allows one to gain important information on atom-atom interactions and quantum statistics in the case of several atoms confined within a single optical (super)well. [S1050-2947(97)03803-1]

PACS number(s): 32.80.Pj, 42.25.Fx, 42.65.−k

An elegant and successful method to cool atoms below the recoil-limit is velocity selective coherent population trapping (VSCPT), which is based on optical pumping of the atoms into a ''dark'' superposition of ground states completely decoupled from the laser fields. This mechanism has been recently demonstrated experimentally yielding extremely narrow velocity distributions in three dimensions (3D) [1]. With respect to realizing Bose-Einstein condensation [2] or building a coherent laserlike source of atoms [3] by pure optical cooling and trapping mechanisms, a major drawback of this scheme consists of its lack of spatial atomic confinement. In order to obtain cooling and trapping simultaneously, an additional confinement mechanism is needed. In this case, no exact dark state can persist, but with properly chosen external potentials, at least in principle, a quasidark ''gray'' state can be achieved and significantly populated [4].

A conceptually different approach is to build gray optical lattices for atoms using a blue detuned standing wave laser field. Such lattices have been experimentally realized and investigated by several groups [5,6]. The atoms are simultaneously cooled and confined periodically in space, but the densities obtained so far are less than one atom per lattice site, precluding the observability of quantum statistical effects and direct atom-atom correlations.

An alternative possibility to trap atoms in a VSCPT configuration is based on the use of *two* pairs of counterpropagating σ_+ and σ_- polarized laser beams [7] of different frequency. In this model both pairs of laser beams simultaneously contribute to the cooling as well as to the trapping of the atoms into large periodical potential wells formed by the beat of the two slightly different laser frequencies. The resulting gray state then is optimally adapted to the laser configuration. This scheme allows much longer lifetimes and a lower mean energy of the trapped atom states as compared to normal gray lattices. In addition, due to the large size of the optical potential wells, occupation numbers of more than one atom per site can be expected, implying a wealth of interesting new physical phenomena [3].

Besides looking at the fluorescence and weak field absorption spectra as discussed recently by Guo and Cooper [8] and measured by various groups [6,9,10], an elegant way to monitor the spatial confinement and temperature of atoms in a lattice consists in the observation of Bragg scattering of a probe laser [11]. In this work we will show a conceptually easy way of measuring the spatial atomic distribution in a dark optical superlattice (i.e., a lattice of periodicity L which is large compared to a single optical wavelength) simply by monitoring the coherently scattered light field of the trapping lasers. This type of scattering can only occur in such a superlattice configuration and can be interpreted as a new kind of Bragg scattering. Hence the system offers a very sensitive, automatically built in monitoring system.

In the following we will solve a simplified 1D model, e.g., we may assume that the atoms are located at a straight line with a small transverse extension. Later we will give an outline of possible extensions to higher dimensions, which provide experimentally more realistic situations.

Let us consider two pairs of counterpropagating σ_+ and σ_- polarized laser beams with wave vectors k_1 and k_2, respectively, corresponding to two distinct $J=1$ to $J=1$ transitions of the atom. For sufficiently large detunings the excited states are only weakly populated and hence can be adiabatically eliminated. As the $m=0$ ground state is efficiently depleted by optical pumping, the model atom can be reduced to its two degenerate $|m=\pm 1\rangle$ ground states. In a rotating frame the Hamiltonian for this system reads

$$H=\hat{p}^2/2m+\sum_{n=1,2} U_n A^n(\hat{x}), \tag{1}$$

where $\hat{p}$ and $\hat{x}$ are the momentum and position operators and $U_n=\frac{1}{2}\Delta_n s_n$ denotes the effective optical potential strength due to the nth laser pair, where Δ_n is the corresponding detuning and s_n the saturation parameter per beam including the Clebsch-Gordan coefficient. The operators A^n are defined as

$$A^n(\hat{x})=[a_+^{n\dagger}(\hat{x})|-1\rangle+a_-^{n\dagger}(\hat{x})|+1\rangle] \times[a_+^n(\hat{x})\langle -1|+a_-^n(\hat{x})\langle +1|] \tag{2}$$

with $a_\pm^n(x)=\exp(\mp ik_n x)$ the mode functions of the respective polarization components of the lasers. Optical pumping occurs due to absorption of a single laser photon and a subsequent spontaneous decay into a $\sigma_\pm$ polarized photon at an angle θ. The corresponding optical pumping operators [13] are $\exp(-ik_n\hat{x}\cos\theta)B_\pm^n(\hat{x})$, where

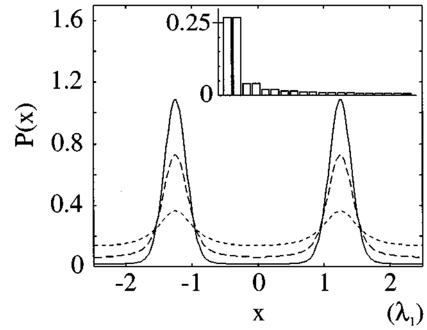

FIG. 1. Position probability of the atom in steady state for two potential wells. The atom is strongly localized at the minima of the adiabatic potential V_-. The parameters are chosen as $U_1=20\omega_R$, $U_2=3\omega_R$, $k_2=1.2k_1$, and $\gamma_2=0.001\gamma_1$ (solid curve), 0.01 (long dashes), 0.1 (short dashes), respectively. The inset shows the occupation probability of the lowest system eigenstates corresponding to the long-dashed curve.

$$B_\pm^n(\hat{x})=a_+^n(\hat{x})\sigma_{\mp -}+a_-^n(\hat{x})\sigma_{\mp +}, \tag{3}$$

and $\sigma_{\pm\pm}=|\pm 1\rangle\langle\pm 1|$. In a semiclassical picture a slow atom would see the so-called adiabatic potentials as obtained by diagonalizing only the second part of the Hamiltonian (1) at each point in space,

$$V_\pm(x)=U_1+U_2\pm\sqrt{U_1^2+U_2^2+2U_1U_2\cos 2(k_1-k_2)x}, \tag{4}$$

yielding a periodicity of the optical lattice of $L=\pi/|k_1-k_2|\gg\lambda$. In steady state the atom is trapped near the minima of V_- with a large fraction of atoms populating the quasidark localized ground state of this potential. Note, however, that for realistic parameters this means an extension over several wavelengths and thus a single-atom model still seems appropriate as a first approximation [12].

For the calculation of the steady state we use a rate equation approach similar to Castin and Dalibard [13]. To this end we numerically diagonalize the Hamiltonian (1) on a spatial grid extended over one or a few superperiods [7].

The stationary spatial distribution for fixed effective light shifts and a few typical values of the effective optical pumping rates $\gamma_n=\frac{1}{2}\Gamma_n s_n$ is depicted in Fig. 1, where Γ_n denotes the atomic linewidth. The inset of Fig. 1 shows the occupation probability of the lowest system eigenstates. For the chosen parameters the lowest energy band, which consists of two eigenstates, contains over 50% of the atomic population, since the lifetime of these states is about one order of magnitude larger than the lifetime of the next energy band (the decay rate is $8.4\times 10^{-4}\gamma_1$ compared to $6.6\times 10^{-3}\gamma_1$). For stronger fields and larger superperiods the ground state occupation can come close to 100% [7]. It is of course an important question if and how these nice properties of superlattices could be observed and experimentally checked. As the central point of this work we will now calculate the coherent part of the spectrum of resonance fluorescence and exhibit how it can be used as a measuring tool to investigate the atomic position and energy distribution in the superlattice [11].

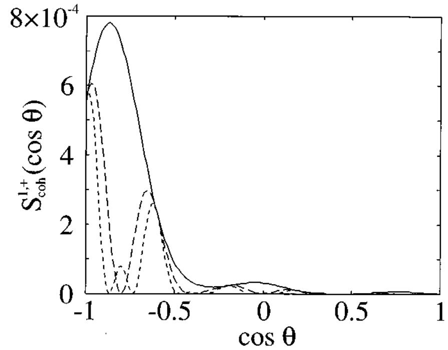

FIG. 2. Angular dependence of the dimensionless coherent spectrum for one polarization component. The emission stems from a single potential well (solid curve), from two wells (long dashes), and from three wells (short dashes), respectively. The parameters are chosen as $k_2/k_1=1.2$, $U_1=20$, $U_2=3$, $\gamma_1=1$, and $\gamma_2=0.01$ in units of ω_R.

The spectrum of resonance fluorescence of $\sigma_\pm$ polarized light is obtained by the Fourier transform of the stationary atomic dipole correlation function, which in our model yields [14]

$$S^{n,\pm}(\Delta,u)=\frac{\omega_R}{2\pi}\int_{-\infty}^{\infty}d\tau e^{-i\Delta\tau}\langle B_\pm^{n\dagger}(\tau)e^{ik_n u\hat{x}(\tau)} \times B_\pm^n(0)e^{-ik_n u\hat{x}(0)}\rangle, \tag{5}$$

where Δ denotes the detuning of the emitted light with respect to the nth trapping laser, $u=\cos\theta$ the emission direction, and ω_R the recoil frequency. Up to a constant prefactor $S^{n,\pm}(\Delta,u)$ gives the number of photons emitted per unit time, per frequency unit, and solid angle.

We will concentrate on the coherent part of the emission spectrum, obtained by factorizing the expectation value in Eq. (5), which gives $S_{\mathrm{coh}}^{n,\pm}(\Delta,u)=\omega_R\delta(\Delta)|\langle B_\pm^{n\dagger}e^{ik_n u\hat{x}}\rangle|^2$.

Let us first look at the radiation emitted from a single potential well, cf. the solid curve of Fig. 2. Due to the position dependence of the phase of the atomic dipole induced by the lattice laser, the forward direction, $\theta=\pi$, for the given polarization component in Fig. 2, contributes most to the coherent spectrum, whereas backward scattering is strongly suppressed. The deviation of the maximum from $\theta=\pi$ is caused by a change of this phase due to the second laser pair.

If we now extend the calculation of the coherent spectrum to include several superperiods, the light emitted from different potential wells interferes constructively or destructively depending on the emission angle. This is a sort of Bragg scattering by the atoms trapped in the periodical potential. As an example, in Fig. 2 we have plotted this spectrum calculated for different numbers of participating potential wells.

The coherently scattered light amplitude from N potential wells in the far field is related to that from a single well by a geometrical structure factor [15] of

$$f(\theta)=\sum_{m=1}^{N}\exp(imk_nL(1-\cos\theta)). \tag{6}$$

The scattered intensity scales with $|f(\theta)|^2$, and therefore the spectrum from N wells is given by

$$S_{\rm coh}^{n,\pm}(\Delta,u)=\omega_R\delta(\Delta)\left|\frac{1}{N}f(u)\right|^2|\langle B_{\pm}^{n\dagger}e^{ik_nu\hat{x}}\rangle|^2, \qquad (7)$$

where $u=\cos\theta$ and the expectation value now has to be taken with respect to the stationary density matrix restricted and normalized to a single superperiod.

In a classical picture for a large number of superperiods the scattered light interferes destructively for most angles and only very sharp peaks occur in directions, where all terms of Eq. (6) add up constructively. This yields the Bragg angles fulfilling $\cos\theta=1-2m\pi/k_1L$, where m is an integer. Inserting the expression for the superperiod L one obtains the following condition: $\cos\theta=1-2m|k_2/k_1-1|$. Hence, for typical wavelength ratios many Bragg resonances can be observed, e.g., at $\cos\theta=-1,-0.6,\ldots$ in Fig. 2.

Note that the photon flux integrated over all emission directions is rather small, of the order of $10^{-4}\gamma_n$ per atom, since in steady state the atom mostly populates the nearly dark ground state. Nevertheless the strong directionality should still allow the observability of the signal as it has been achieved for ordinary optical lattices [6].

The beauty of the presently discussed bichromatic trap is that the trapping lasers themselves act as sensitive as probe beams. It is possible to observe Bragg scattering from the trapped atom without any additional probe laser disturbing the system. This only works because the periodicity in this model is larger than the wavelength of the trapping lasers, in contrast to ordinary optical lattices built with a single laser wavelength spectrum one intricate [11]. In our model this diagnostic tool is automatically built in, which means that we do not have to introduce an external perturbation for the measurement and thus the physical situation remains as ''clean'' as possible.

As is well known from solid state physics [15] the Bragg spectrum provides sensitive information on the spatial extension of the scatterers (Debye-Waller factor), which in turn allows one to obtain the occupation probability of the lowest energy levels. We demonstrate this explicitly for our lattice in Fig. 3, where we plot the relative intensity R of the first Bragg peak relative to the second, the root mean square of the spatial distribution, and the ratio of the atomic populations of the first excited state p_1 and of the ground state p_0, which show clear correlations.

For smaller values of γ_2 the ground state occupation increases [7], since optical pumping on this second transition is mostly responsible for the decay of the ground state. This yields a stronger localization of the atom, see also Fig. 1, and thus the emission spectrum is more homogeneous, which is manifested in the relative height of different Bragg orders. [According to Eq. (7) an atom in a position eigenstate $|x\rangle$ would give a completely flat spectrum.] From Fig. 3 it can be seen that there exists a one-to-one correspondence between these quantities. Hence the relative intensity of different Bragg orders provides an experimentally accessible measure of some properties of the stationary population distribution. For instance, from the ratio p_1/p_0 derived in this way one can obtain an estimate for the system temperature, although, strictly speaking, there is no well-defined temperature since the steady state population distribution is far from a thermal one.

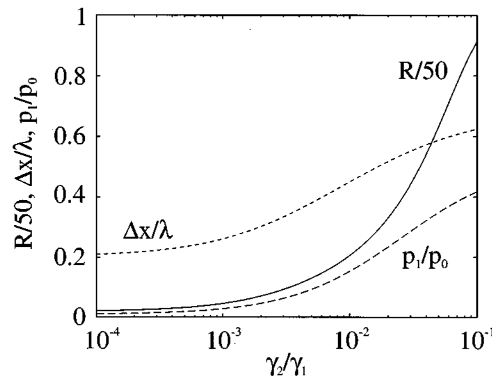

FIG. 3. Relative height of the first to the second order Bragg peak R (solid curve), root mean square of the spatial distribution of the atom within a single potential well Δx (short dashes), and ratio of the populations of the lowest states p_1/p_0 vs γ_2. The parameters are the same as in Fig. 2.

So far we restricted ourselves to a quasi-one-dimensional model where the atoms are strongly localized in the transverse directions. Experimentally it is more realistic to consider a 2D or 3D lattice setup. Unfortunately, it is not possible to perform all the numerical calculations analogous to 1D due to the size of the Hilbert space. However, by looking at the adiabatic potentials we can argue that the proposed scheme also works in higher dimensions, as we will show in the following. The basic principle remains the same as in 1D: for any appropriate laser configuration there exists a dark state consisting of a few plane wave components in an atomic $J=1$ to $J=1$ transition [1,16]. By ''doubling'' this configuration (using two frequencies) in the same sense as in 1D one obtains a superlattice structure with potential minima of zero light shift. Figure 4 shows a contour plot of the lowest adiabatic potential in a rectangular 2D configuration.

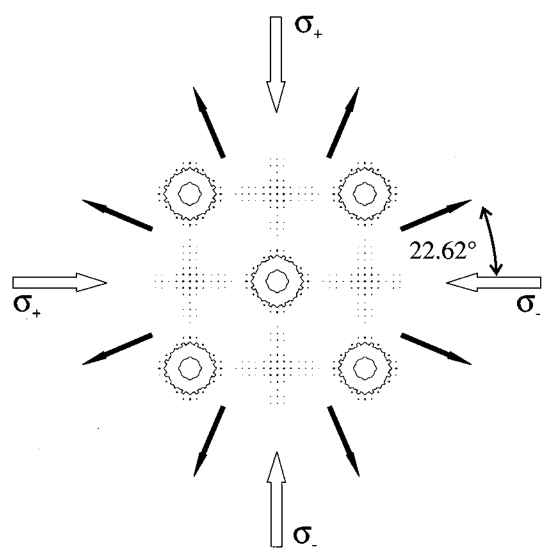

FIG. 4. Rectangular 2D configuration for a superlattice for the parameters of Rb atoms ($L=26\lambda_1$). The white arrows represent the various trapping lasers and the black ones indicate the possible Bragg scattered beams. In the center of the figure a contour plot of the lowest adiabatic potential is given. The optical potentials are chosen as $U_1=50\omega_R$ and $U_2=10\omega_R$.

The Bragg conditions for such a lattice can be derived easily by considering the reciprocal lattice [15]. Again coherent scattering of the trapping lasers will occur only for certain angles, which can be changed by adjusting the directions and frequencies of the involved laser fields, e.g., by a deviation from the rectangular setup and/or by introducing a small angle between the lasers of different wavelengths. In general it is a nontrivial problem to find the corresponding angles. As an example for Rb atoms ($\lambda_1 = 795$ nm, $\lambda_2 = 780$ nm, $L = 26\lambda_1$), a simple rectangular setup yields several Bragg angles, as depicted in Fig. 4. Thus for this case the proposed scheme of measuring the Bragg scattered trapping lasers as a diagnostic tool also works in 2D and similarly in a 3D extension.

In conclusion, we have shown that an optical superlattice created by a bichromatic laser field produces a Bragg spectrum of the trapping lasers themselves, which can be used to measure and analyze the atomic state. Hence, in contrast to other schemes, this system automatically provides its own diagnostic tool, without the need for any additional probe lasers. The superperiod of the lattice can be deduced from the Bragg angles, while simultaneously the relative heights of different Bragg orders give an indication of the level occupation probabilities and spatial confinement.

A central motivation to construct such a superlattice is the prospect of achieving densities of more than one atom per well starting from an initial density as one obtains in a standard MOT. Hence atom-atom interactions at very low temperatures and a low number of scattered photons including quantum statistical effects should play an important role. In this case via the Bragg spectrum discussed in our work one could sensitively monitor the time dependent changes in the spatial atomic distribution as a function of the initial density (number of atoms per well). From these quantities one could deduce information on the interatom interaction strength and the quantum statistical correlations of different atoms occupying the same trapping state. This could be of great value for similar setups, which are theoretically discussed as possible candidates for building a laserlike source of atoms [3,17,18].

This work was supported by the Österreichischer Fonds zur Förderung der wissenschaftlichen Forschung under Project No. S06506-PHY. We want to thank A. Hemmerich for helpful discussions.

[1] J. Lawall *et al.*, Phys. Rev. Lett. **75**, 4194 (1995).
[2] M. H. Anderson *et al.*, Science **269**, 198 (1995); C. C. Bradley *et al.*, Phys. Rev. Lett. **75**, 1687 (1995); K. B. Davis *et al.*, *ibid.* **75**, 3969 (1995).
[3] R. J. C. Spreeuw *et al.*, Europhys. Lett. **32**, 469 (1995).
[4] R. Dum *et al.*, Phys. Rev. Lett. **73**, 2829 (1994); T. Pellizzari, P. Marte, and P. Zoller, Phys. Rev. A **52**, 4709 (1995).
[5] G. Grynberg and J.-Y. Courtois, Europhys. Lett. **27**, 41 (1994).
[6] A. Hemmerich *et al.*, Phys. Rev. Lett. **75**, 37 (1995).
[7] T. Pellizzari and H. Ritsch, Europhys. Lett. **31**, 133 (1995).
[8] J. Guo and J. Cooper, Phys. Rev. A **52**, R1819 (1995).
[9] P. Verkerk *et al.*, Phys. Rev. Lett. **68**, 3861 (1992).
[10] P. S. Jessen *et al.*, Phys. Rev. Lett. **69**, 49 (1992).
[11] M. Weidemüller *et al.*, Phys. Rev. Lett. **75**, 4583 (1995); G. Birkl *et al.*, *ibid.* **75**, 2823 (1995).
[12] E. Goldstein *et al.*, Appl. Phys. B **60**, 161 (1995).
[13] Y. Castin and J. Dalibard, Europhys. Lett. **14**, 761 (1991).
[14] P. Marte *et al.*, Phys. Rev. Lett. **71**, 1335 (1993); P. Marte, R. Dum, R. Taïeb, and P. Zoller, Phys. Rev. A **47**, 1378 (1993).
[15] See, e.g., N. W. Ashcroft and N. D. Mermin, *Solid State Physics* (Saunders College Publishing, Philadelphia, 1976).
[16] M. A. Ol'shanii and V. G. Minogin, Quantum Opt. **3**, 317 (1991).
[17] J. I. Cirac, M. Lewenstein, and P. Zoller, Phys. Rev. A **50**, 3409 (1994).
[18] H. M. Wiseman and M. J. Collett, Phys. Lett. A **202**, 246 (1995).